JOURNAL OF MATERIALS SCIENCE 13 (1978) 722–730

The fracture toughness of reinforced polyurethane foam

T. COTGREAVE, J. B. SHORTALL
Department of Metallurgy and Materials Science, University of Liverpool, UK

A microscopic study of the fracture processes occurring in rigid, closed-cell polyurethane foam has been combined with an assessment of toughness using fracture mechanics in order to investigate the reinforcement capability of chopped glass fibres. One aspect of fibre reinforcement is seen as an extension of a mechanism that could be responsible for the relatively high surface energy of the base foam. There is also an increase in modulus, and a further contribution to toughness is derived from fibre pull-out. An optimum, though unspecified, fibre length exists that gives the most efficient reinforcement of the foam considered.

1. Introduction

The advantages of using rigid foamed plastics, which include lower material costs, lighter weight structures, high strength to weight ratios and versatility in processing, are becoming of increasing importance in the polymer industry. The continued desire to improve the properties of these foams, which may be required to withstand demanding environmental conditions, provides an incentive for seeking means of reinforcing the basic matrix.

In an earlier paper [1] a mechanism of reinforcement of rigid polyurethane foam by high modulus chopped fibres was described. When incorporated into the foam, a fibre formed the core of an elongated composite strut; the effective interface in this system was the array of radial struts based on the composite strut that attached it to the bulk matrix. Destructive tensile loading of the foam resulted in shear of the radial struts which produced a unique form of pull-out fragment characteristic of the system. The generation of pull-out fragments was subject to the usual constraints of critical fibre length and an expression for calculating this, denoted as l_{cm} for a matrix-limited foam system in which failure occurs in a region remote from the fibre surface, was derived. The modes of failure observed and the generation of pull-out fragments indicated a potential toughening mechanism.

1.1. Fracture mechanics considerations

The use of fracture mechanics to describe the toughness of engineering materials is often centred on the determination of the critical stress intensity factor K_{IC} (in which the subscript I denotes the crack opening failure mode). It represents a measure of the elastic stress field induced in a cracked body by an applied load in the vicinity of the crack tip and which will result in crack extension. Thus it reflects the resistance to brittle fracture of the material [2]. The basic concepts presuppose the existence of an inherent or induced crack or flaw in the material and relate the magnitude of such a crack and the stress intensity factor to the failure stress of the specimen. A brittle material is sensitive to the size of an initial crack whereas the reduction in strength caused by a crack in a tough material is proportional only to the reduction in cross-sectional area occasioned by its presence.

Fracture mechanics concepts were originally formulated to account for brittle failure in flawed single-phase materials. One of the aims of reinforcing a brittle matrix is to improve its toughness which, on the basis of elementary theory, should render a fracture mechanics treatment inapplicable. Recently however, the fracture properties of certain composite materials have also been successfully explained [3–7] using the standard formulae derived for isotropic materials.

© *1978 Chapman and Hall Ltd. Printed in Great Britain.*

1.2. Fracture of polyurethane foam

Closed-cell rigid polyurethane foam is a three-dimensional space frame structure with the cells bonded by clearly defined resin struts and enclosed by thin resin membrane windows. It might be expected that a complex fracture pattern would result from the multidirectional orientation of the struts which are the major load bearing elements. However, on a macroscopic scale, the tensile fracture of unreinforced polyurethane foam is a rapid process and the resultant fracture surface is essentially planar. The brittle nature of the failure suggests that fracture mechanics could be used to characterize the fracture toughness of polyurethane foam and this approach has been validated and used to give estimates of characteristic flaw size [8, 9]. This has been found to approximate to the mean cell diameter.

The tensile fracture surface of fibre reinforced polyurethane foam is non-planar and discrete pull-out fragments dominate its appearance [1]. In general the matrix crack does not propagate through to the fibre surface but instead is diverted through the radial struts bounding the first layer of foam cells based on the composite strut that embodies the fibre.

The objective of the work presented here was to identify the effect of fibre reinforcement on the fracture toughness of rigid polyurethane foams. In this paper the fracture properties of rigid polyurethane foam are explored and the effects of fibre reinforcement are quantified using a fracture mechanics approach.

2. Experimental

2.1. Materials

Rigid closed-cell polyurethane foam was prepared from a "Caradol-Caradate" blend supplied by Shell Chemicals (UK) Limited, using trichlorofluromethane as blowing agent. Low-density ($35\,kg\,m^{-3}$) foam, both reinforced and unreinforced, was used in a detailed study of the fracture processes, and high-density foam ($80\,kg\,m^{-3}$) was used in the measurement of fracture properties. The latter was produced by spraying, both as an unreinforced foam, and reinforced with chopped glass fibres which were incorporated by projecting them directly from a chopper fed with glass roving. The rovings, supplied by Pilkington Research Laboratories, were treated with a size which is nominally non-compatible with polyurethane, but allowed a favourable fibre distribution at two different concentrations (approximately 1.0 and 0.7 wt%). The lower size concentration allowed a proportion of individual filaments to separate from the roving whereas no filamentization occurred at the higher concentration. The fibres treated with the more usual (1.0 wt%) size concentration were chopped to 12 mm and the fibres with the lower size concentration were used at 5, 12, 20 and 40 mm lengths.

2.2. Microscopy

Specimens of the low-density foam approximately 60 mm x 15 mm and 1 to 2 mm thick were cut on a low speed "Isomet" diamond wafering saw running in a light petroleum spirit and the foam debris was removed by ultrasonic cleaning in a similar solvent. The specimens were placed in a miniature tensioning jig fitted to a Riechert polarizing microscope and observed in reflected light. The fracture sequences were "frozen" at various stages by relaxing the load to permit photography.

Specimens of the reinforced foam which had fibres aligned with the tensile axis were selected for a study of the effects of the presence of the fibre on the deformation processes.

2.3. Fracture toughness testing

The higher density foams were cut on a high-speed diamond saw to give rectilinear specimens, 200 mm x 80 mm x 20 mm, as shown in Fig. 1. A central hole approximately 3 mm diameter was drilled through the major face and a notch of total length 30 to 40 mm was extended symmetrically from

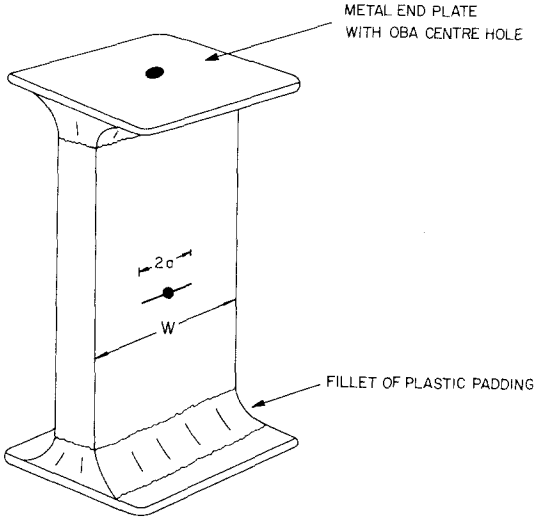

Figure 1 Specimen for K_{IC} determination.

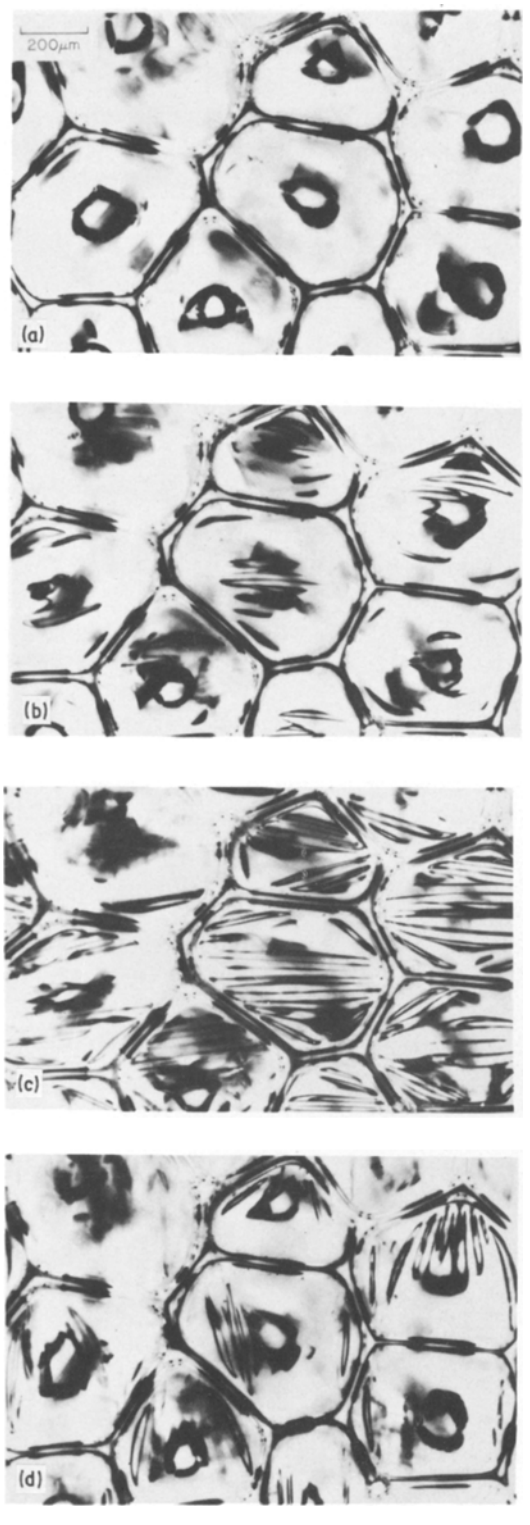

Figure 2 (a) Structure of plain foam, relaxed state; (b) structure under tension showing windows starting to buckle; (c) high degree of window buckling with splitting imminent; (d) plane of buckling changed under slight compression.

the hole in the width direction with a fine saw. The crack tips were sharpened using a razor blade. The ends of the specimen were bonded to metal plates with Plastic Padding (Plastic Padding Ltd., High Wycombe, Bucks.) before testing in an Instron machine at a cross-head speed of $10\,mm\,min^{-1}$.

3. Results

3.1. Low density foam

The low-density foam specimens were subjected to tensile loading in the miniature testing jig and observed under the microscope. The initial deformations observed corresponded to a "lazy-tongs" action as the space frame structure formed by the cell struts was extended in the direction of the tensile axis, each cell unit showing pronounced longitudinal extension and lateral contraction resulting from flexure of the non-aligned struts. The cell windows formed between the struts also stretched along the tensile axis and buckled in the transverse direction. At low loading, these processes appeared as reversible elastic deformations. Fig. 2a shows the foam in its initial state and Figs. 2b and c show stages of increasing tension. In Fig. 2d the loading has been changed from tension to compression to show the cell windows buckling in the opposite plane.

At higher tensile loadings the buckled cell windows started to tear and the cracks propagated to notch an adjoining strut. Fig. 3a shows the early stages of crack development, and the notch in the strut was seen to grow in a controlled manner with increasing load through one third of the strut's discernable diameter, as in Fig. 3b, before it failed completely. The crack progressed rapidly across the next window to another strut where the notching process was repeated.

On several occasions it was noted that a crack propagating through a window was directed to a node formed at the junction of struts. Here the notching effect was minimal and the crack progressed no further at that particular front. This situation is shown in Fig. 3c. Instead, a new front was created at either a different site in the same cell window or at a site in a neighbouring cell.

Microscopic examination of sections taken from the fracture surface of foam specimens that had been broken in tension showed fracture patterns that were consistent with this form of crack arrest and regeneration having taken place throughout the whole of the fracture zone. Fig. 4 shows a

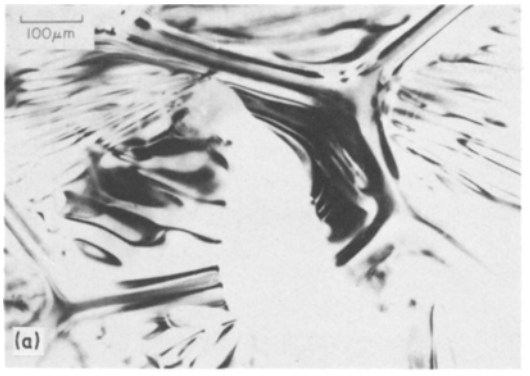

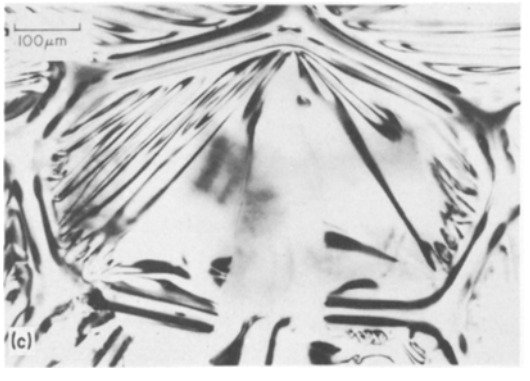

Figure 3 (a) Crack path across a cell and a notched strut; (b) notch grown through a third of the strut's diameter; (c) crack arrest at a node formed at the junction of struts.

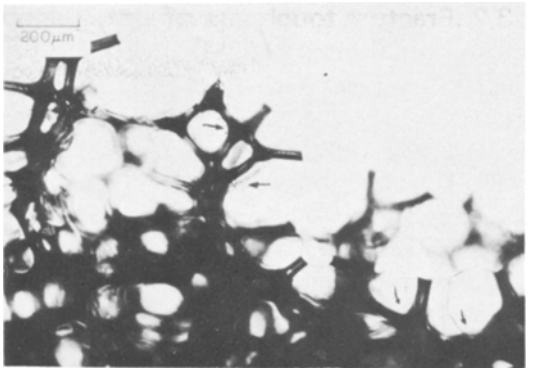

Figure 4 Section of the tensile fracture surface showing crack arrest points (arrowed).

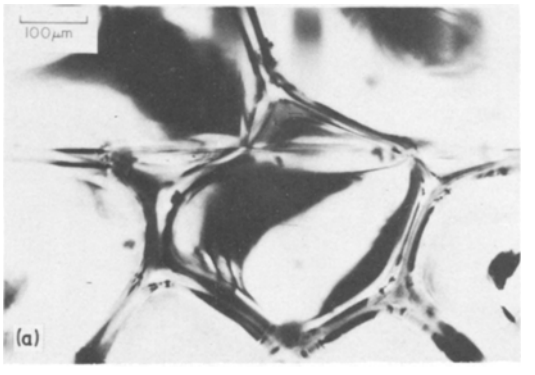

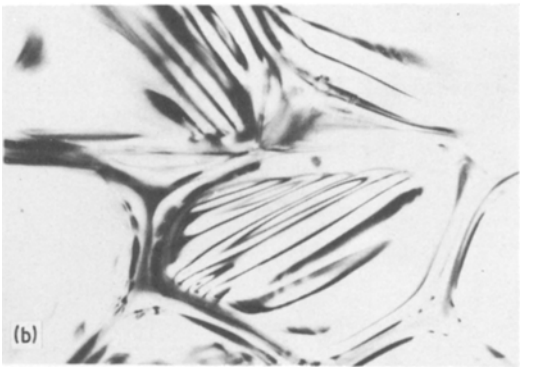

Figure 5 (a) Cells based on a single filament, (b) buckling pattern in cells on a filament.

number of crack arrest sites in a section taken from a fracture surface. Any attempt at assessing the frequency with which "node arrest" occurs, in comparison with the normal propagation of a crack across a cell, must at this stage be largely subjective. However, the available evidence suggests that node arrest was occurring in the 35 $kg\,m^{-3}$ foam at one cell in ten.

A fibre in the reinforced foam becomes a long composite strut that is incorporated into the foam during its formation and locally modifies the foam strut matrix by creating an alignment of the cells which surround it as shown in Fig. 5a. These cells, which thus have a common base, are effectively braced against the laze tongs type deformation, occurring during tensile loading, which is seen in the free foam. Evidence for this can be seen in Fig. 5b in which the windows attached to the composite strut show asymmetric buckling compared with the uniform buckling across each window of the free foam shown in Fig. 2c.

3.2. Fracture toughness of unreinforced and reinforced foams

The test specimen dimensions were chosen to maintain plane strain conditions during tensile fracture [10]. This gives a more conservative estimate of fracture toughness than the plane stress state prevalent in thin sections. The absence of noticeable shear lips on the fracture surfaces of the specimens confirmed that the required conditions were maintained.

Under an increasing load, a crack will grow in an unstable manner when the stress intensity factor K_I reaches a critical value K_{IC} and will continue to propagate for as long as $K_I \geqslant K_{IC}$, provided that general yielding does not occur. In practical terms, for polyurethane foam, this translates as virtually continuous rapid crack growth from initiation to complete specimen failure. The failure stress under the prevailing conditions can be calculated from the peak value attained in the stress/strain curve.

$$\sigma = \frac{P}{BW} \tag{1}$$

where σ = failure stress (kN m^{-2}),
P = load at failure (kN),
B = specimen thickness (m),
and W = specimen width (m).

The critical stress intensity factor represents the stress distribution at the crack tip for the given specimen configuration and can be calculated from the failure stress, the dimensions of the specimen and the induced crack using the equation:

$$K_{IC} = \sigma\sqrt{(\pi a)}H, \tag{2}$$

where H is a "shaping factor" tabulated for various initial crack length to specimen width ($2a/W$) ratios [11]. This factor varied from 1.06 to 1.08 for the specimen dimensions used. The creation of the fracture surfaces can be described by a corresponding energy term and critical strain energy release rate (G_{IC}) values may be derived from K_{IC} data (plane strain) and Young's modulus (E) values as as follows:

$$G_{IC} = K_{IC}^2(1 - \nu^2)/E \tag{3}$$

where ν is Poisson's ratio which is 0.3 for the foam used.

Table I shows consistent K_{IC} results for specimens of reinforced foam at two crack length to specimen width ratios and supports the use of K_{IC} measurements at least as a comparative method for assessing the effects of fibre reinforcement of polyurethane foam.

In Table II, the mean K_{IC} values for reinforced foams containing essentially the same weight fraction of glass fibres are presented together with the toughness values for the unreinforced foam. Also included are the measured modulus values and the calculated G_{IC} values.

It is evident that the presence of fibres of any of the lengths considered causes some increase in K_{IC}; however, it is perhaps more instructive to look at the individual test results and the fibre concentration. Each pair of fracture surfaces supported a particular population of fibres that had been involved in the fracture processes.

Fig. 6a shows a plot of measured fracture toughness values against fibre population for the 12 mm fibres. Despite the scatter in results there is a general trend; the fibres treated at the normal size concentration and at the low size concentration falling on the same line. Similar plots are obtained for the 5, 20 and 40 mm fibres, at low size concentration, which are shown in Figs. 6b, c and d respectively. Although the linear relationship drawn through the origin that is shown for the 40 mm

TABLE I K_{IC} measurements on reinforced foam at two crack length to width ratios

$2a/W$	K_{IC} (kN m$^{-3/2}$)
0.30	126
0.40	128

TABLE II Comparison of fracture properties

Fibre type	Number of fibres per unit area (Fibre cm^{-2})	K_{IC} (kN m$^{-3/2}$)	E (MN m^{-2})	G_{IC} (N m^{-1})
Unreinforced	0	101	19.1	486
12 mm, 1.0 wt% size	4.3	124	27.4	511
12 mm, 0.7 wt% size	7.6	146	34.0	571
5 mm, 0.7 wt% size	13.7	130	27.9	551
20 mm, 0.7 wt% size	4.8	130	35.4	434
40 mm, 0.7 wt% size	5.1	116	30.3	404

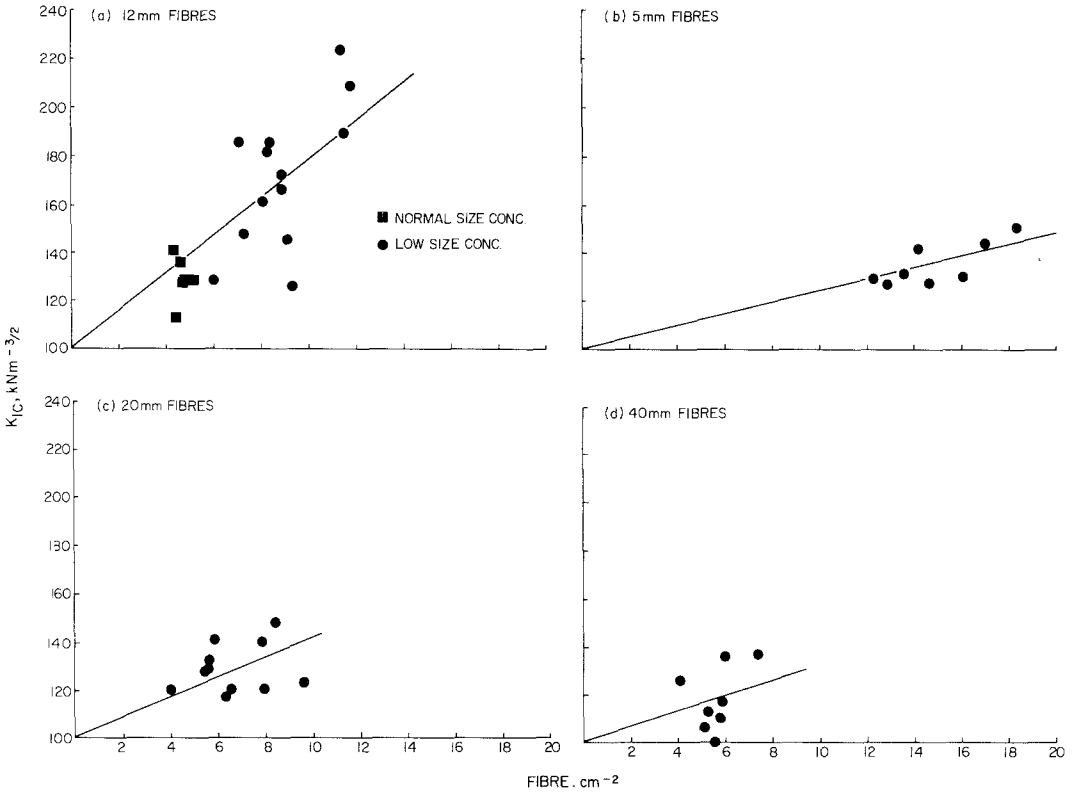

Figure 6 Fracture toughness versus fibre concentration.

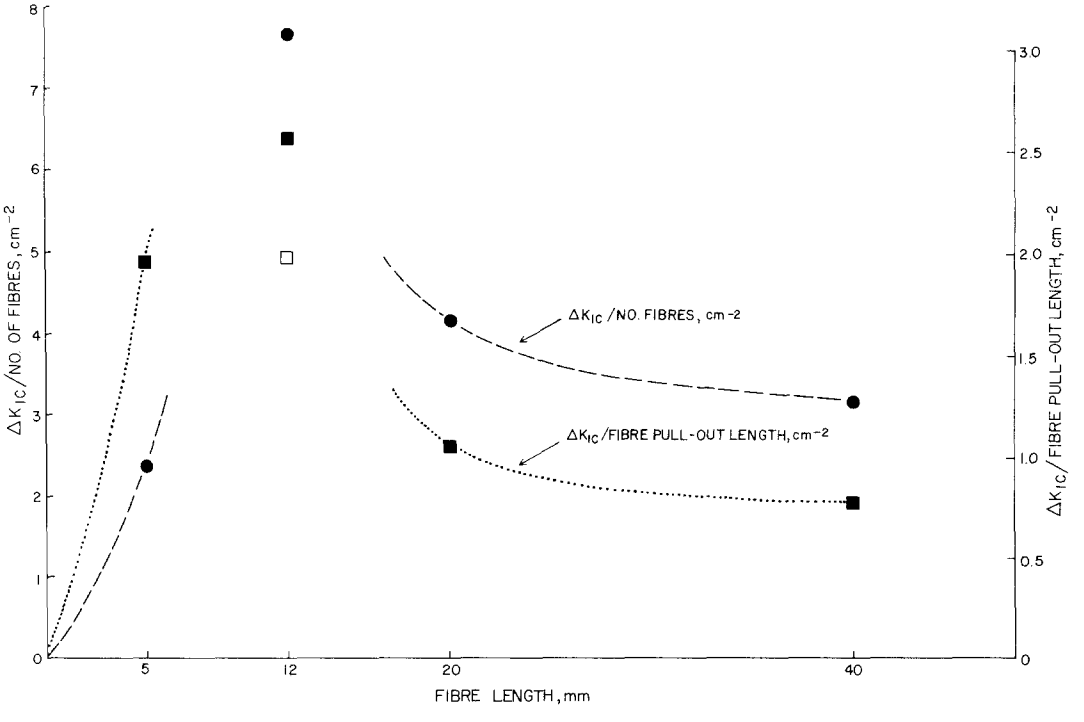

Figure 7 Coefficient of reinforcement for different fibre lengths.

fibres would appear somewhat tenuous, it is included for comparison reasons. In fact, to draw a "best" straight line relationship through the points available would imply the existence of negative toughness values at very low fibre concentrations. A nonlinear relationship reflecting a reduced toughness arising from stress concentrations due to the presence of a few fibres is also possible. However this effect is not observed at comparable fibre concentrations in Figs. 6a and c and the distribution of data points in Fig. 6d is more likely due to the experimental error associated with the test and the reproducibility in material preparation.

From the slope of the lines through the various sets of points an estimate of the efficiency of reinforcement can be obtained for the different fibre lengths. A "coefficient of reinforcement" may be defined as the increase in fracture toughness per fibre per square centimetre; when this is plotted against initial fibre length the result is as shown in Fig. 7. An equivalent expression based on the total fibre pull-out length per square centimetre produces a similar curve. The open square symbol is the corresponding plot for the 12 mm fibres with the higher size concentration and it indicates a lower efficiency by the non-filamentized glass which was not apparent from the simple fibre concentration plot in Fig. 6a.

4. Discussion

Rigid closed-cell polyurethane foam is a finely structured material in which the cells are bounded by the major load-bearing elements, the well defined solid resin struts, and enclosed by very thin resin windows. It may be expected that the resultant, complex, three-dimensional structure might behave somewhat differently under destructive loading than will a solid isotropic system.

The basic modes of failure have been described previously [12] and it has been shown that the windows play a major part in crack initiation under tensile loading. The resultant strut notching is reported to be a factor responsible for the reduced tensile strength of a closed-cell foam compared with that of a similar reticulated foam. However, these values remained within the same order of magnitude and are close to the values that can be calculated from the strength of the solid polymer on a density reduction basis.

More recently, the outstanding surface energy to strength ratio of polyurethane foam compared with those of solid systems has been highlighted [8], and it follows that a high surface energy is responsible for placing this ratio for the foam an order of magnitude higher than the others. It has also been suggested that the cellular spaces act as crack arrestors and thus give rise to a high surface energy but whilst this is undoubtedly true for a reticulated foam, the work reported here shows that in a closed-cell foam, the cell window acts as a continuum that facilitates crack propagation from strut to strut and thus counters the effect of the open space in the cell. On the other hand there is evidence that a moving crack is often directed across a window to the node formed at the junction of struts and there becomes arrested. A new crack must then be initiated at an adjacent site for the failure process to continue. Based on the frequency of occurrence of "node arrest", it is suggested that this is a major factor contribution to the high surface energy of closed cell polyurethane foam. This has a direct bearing upon the mechanism by which chopped fibres can reinforce the foam. The primary function of a fibre in a toughening role is to create a crack arrest and diversion mechanism; this has been shown to occur in practice and its action may be likened to that of a node but having an effect over the entire length of the fibre, thus extending the inherent toughening mechanism of the foam matrix. The presence of fibres of all lengths can be seen to impart an increase in the measured K_{IC} values of the foam; there is also a marked increase in modulus. This results in the calculated G_{IC} values in many cases showing no increase over that of the base foam. Increases in G_{IC} are seen only for those foams containing higher concentrations of fibre. At low fibre concentrations, the extra work due to increased surface area and fibre pull-out and the small number of single filament fractures are insignificant compared with the work of fracture of the matrix. The strain energy release rate for diverting a crack from a path normal to the tensile axis is no greater than that for the normal crack progression [13, 14] and it may even be reduced as the failure mode changes locally from tension to shear. The net effect would be a reduction in overall surface energy, as shown for instance in the case of the 40 mm fibres. In a conventional solid matrix composite, the work of debonding and fibre fracture make important contributions to the surface energy, as shown for instance in the case of the debonding is absent and essentially only isolated

single filaments can fracture, the crack path is confined to the matrix and this is reflected in the surface energy values derived. The small increase in surface area occasioned by the presence of the fibres is insufficient to make a noticeable contribution to the total work of fracture. It is not until sufficient work of pull-out is generated at the higher fibre concentrations, as in the case of the filamentized 12 mm and 5 mm fibres, that a higher surface energy is achieved.

Comparing the 12 mm fibres at the two different size concentrations it can be seen from Fig. 6a that both types lie on the same toughness versus fibre concentrations line. The major difference is that the lower size concentration allows a higher degree of filamentization, and therefore the overall concentration of reinforcing elements, fibre bundles and single filaments, is greater. Whereas some 40% of the reinforcing elements in the latter case are single filaments, there are virtually no filaments produced from the higher size concentration, it is therefore assumed that the toughness-reinforcing potential of a fibrous element is independent of the form of the fibre, and in terms of efficiency of glass reinforcement single filaments and very small bundles are to be preferred [1]. The rovings treated with the low size concentration, which favours filamentization, were used in subsequent experiments to produce the 5, 20 and 40 mm fibres.

The curves expressing the reinforcement capability of the different fibre lengths indicate that a maximum exists at or near the 12 mm length. This is in the region of the critical fibre length for the foam and would allow for maximum pull-out length of the single filaments present. On this basis it may be expected that the longer fibre bundle lengths would be even more efficient, since there is potentially a longer pull-out length available. The work of pull-out, γ_p, for conventional composite systems is given by:

$$\gamma_p = \frac{V_f \sigma_f l^2}{12 l_c} \quad (l < l_c) \tag{4}$$

$$\gamma_p = \frac{V_f \sigma_f l_c^2}{12 l} \quad (l > l_c) \tag{5}$$

From the definition of critical length, l_{cm}, for a single filament in a matrix limited foam system [1] and the characteristic morphology of the composite, it follows that the critical length for a fibre bundle is basically the product of the critical length of a single filament and the number of filaments in the bundle. Whilst this simple relationship must be modified to account for the strength distribution of the filaments and the increased shear zone diameter, the value for the critical length of a bundle remains very large. Therefore in each of the foam composites produced which all contained a major proportion of multi-filament bundles, it could be expected that $l \ll l_{cm}$ and that γ_p should increase in direct proportion to l^2 (Equation 4). Evidence from the present work suggests that this is not the case and therefore some other effect that cancels the pull-out mechanism must be sought.

In the foregoing discussion all the fibres have been treated as being aligned with the tensile axis whereas in practice, in a sprayed foam system, the fibres are randomly arrayed in two dimensions. For crack arrest and diversion and fibre pull-out, all fibres except those lying parallel to the crack path are effective. Considering now the effect that mis-aligned fibres will have on the modulus of the foam, it can be seen that even very small bundles of the shorter fibres will be sufficiently stiff to maintain an effective contribution whereas a similar bundle of longer fibres of the same total length can flex to re-align itself in the relatively weak matrix. There will be a corresponding lesser increase in composite modulus before the matrix fracture strain is locally exceeded and failure occurs. This effect can be seen in Table III in which the percentage increase in modulus per unit fibre length traversing a unit cross-section is given. The lowest modulus is attributed to the longest (40 mm) fibres. The low value for the 5 mm fibres is due to the single filaments present, which are below the critical fibre length (l_{cm}), and which do not achieve maximum strain before matrix failure.

A futher factor, which could result in a lower modulus when longer fibres are used, is that such fibres have a reduced tendency to remain straight.

TABLE III Foam modulus values as a function of fibre length

Fibre length (mm)	$\%\Delta E$ ($MN\,m^{-2}$)	Total fibre length per cm^2 (mm)	$\%\Delta E$/ Fibre length
5	8.8	68.5	0.13
12	14.9	91.2	0.16
20	16.3	96.0	0.17
40	11.2	204.0	0.05

This effect is aggravated by physical interaction between neighbouring and crossing fibres as they are disturbed by the action of the rising foam. A curved fibre would have to straighten before it contributed significantly to the modulus of the foam and again matrix failure could occur before this point is reached.

5. Conclusions

Rigid closed-cell polyurethane foam has an intrinsic toughening mechanism arising from microstructural features that provide for multiple arrests and diversions to occur along the path of a propagating crack. The incorporation of glass fibre reinforcement provides an extension of this natural mechanisms. Also, there is an increased probability of crack interception.

The fibres also serve to increase the modulus of the foam and this results in higher fracture toughness values even though the fracture surface energy, in many cases, shows no increase. Some contribution to the fracture toughness may be attributed to the work required to the extract the unique "pull-out" fragments which characterize the composite.

The fracture toughness of the composite is directly proportional to the fibre concentraion and this can be enhanced by choice of fibre surface treatment. The efficiency of reinforcement varies with fibre length and the existence of an optimum length is indicated.

References

1. T. COTGREAVE and J. B. SHORTALL, *J. Mater. Sci.* **12** (1977) 708.
2. L. P. POOK, "Designers Guide to Fracture Mechanics", N.E.L., (1975) p. 2.
3. D. C. PHILLIPS and A. S. TETELMAN, *Composites*, **9** (1972) 216.
4. P. W. R. BEAUMONT, *J. Adhesion* **6** (1974) 107.
5. G. C. SIH, E. P. CHEN and S. L. HUANG, *Eng. Fract. Mech.* **6** (1974) 343.
6. M. D. SNYDER and T. A. CRUSE, *Int. J. Fract.* **11** No. 2 (1975) 315.
7. M. L. SONI and M. STERN, *ibid* **12** No. 3 (1976) 331.
8. C. W. FOWLKES, *ibid* **10** No. 1 (1974) 99.
9. G. E. ANDERTON, *J. Appl. Polymer Sci.* **19** (1975) 3355.
10. W. F. BROWN and J. E. SRAWLEY, ASTM publication, STP 410, (1966).
11. P. C. PARIS and G. C. SIH, ASTM publication, STP 381 (1964) p. 41.
12. E. A. BLAIR, Resinography of Cellular Plastics, ASTM publication, STP 414 (1967) p. 84.
13. N. L. HARRISON, *Fibre Sci. and Tech.* **5** (1972) 197.
14. *Idem, ibid* **6** (1973) 25.

Received 27 April and accepted 8 July 1977.